



Habitat heterogeneity enhances megafaunal biodiversity at bathymetric elevations in the Clarion Clipperton Fracture Zone

Katja Uhlenkott^{1,2} · Erik Simon-Lledó³ · Annemiek Vink⁴ · Pedro Martínez Arbizu^{1,2}

Received: 12 July 2022 / Revised: 27 February 2023 / Accepted: 3 March 2023 / Published online: 19 July 2023
© The Author(s) 2023

Abstract

The Clarion Clipperton Fracture Zone (CCZ) in the northeast Pacific is a heterogeneous deep-sea environment, featuring abyssal plains as well as multiple seamounts and abyssal hills (bathymetric elevations) that harbour a highly diverse megabenthic fauna. Based on the analysis of seafloor photographic transects that were taken from elevated areas downslope into the abyssal plains in the eastern CCZ, a similar distribution of habitats was observed on five different bathymetric elevations including abyssal hills as well as the foothills of two seamounts. Rock outcrops occur at the summits, surrounded by an area with varying coverage and size of polymetallic nodules, which were divided into two different habitats characterized by large and small nodules, respectively, and followed by nodule-free sediments. Megafauna composition, density and diversity varies across these habitats. While density is the highest in areas with rock outcrops (1.4 individuals per m²), the biodiversity is the highest when regarding all of the habitats combined. Regarded individually, nodule-covered areas are the most diverse, whereas sediment areas without hard substratum, i.e. nodule free sediments, show the lowest biodiversity and the lowest density (0.2 individuals per m²). The multinomial species classification method (CLAM) shows that most of the observed megafauna morphotypes have to be regarded as rare. The large differences between the megafaunal communities at bathymetric elevations and the abyssal plain reported from previous studies might partly be explained by the multiplicity of habitats. This high heterogeneity can lead to a more diversified community at elevations, although most habitats can also be observed in the abyssal plain.

Keywords Megafaunal density · CCZ · Abyssal hills · Seamounts · Polymetallic nodules · Rock · Photographic survey

Introduction

In the past, a common perception of the deep sea was a vast, desert-like plain covered by soft sediments (Ramirez-Llodra et al. 2011). However, this perception was largely based on

knowledge gaps on the abyssal environment, as the biodiversity of benthic communities in the deep sea is, in fact, amongst the highest on our planet (Ramirez-Llodra et al. 2010). Although highest numbers of individuals as well as different species are usually small invertebrates of meio- and macrofauna size (range of micrometers to millimeters) due to decreasing availability of energy with depth (e.g. Rex et al. 2006; Ramirez-Llodra et al. 2010; Durden et al. 2019), megafauna also show high numbers of different taxa and a significant contribution to biodiversity in the Clarion Clipperton Fracture Zone (CCZ) (e.g. Amon et al. 2017; Simon-Lledó et al. 2019b, 2020).

Habitat heterogeneity is considered to be one of the main drivers of biodiversity, as structurally complex environments can provide more niches and thus support a higher species richness (Tews et al. 2004). This ‘habitat heterogeneity hypothesis’ is one of the cornerstones of ecology (MacArthur and MacArthur 1961) and has therefore been tested in various deep-sea ecosystems, such as continental margins (e.g. Levin et al. 2010; Jones and Brewer 2012), seamounts (e.g. Bell et al. 2016), canyons (e.g. McClain

Communicated by T. Horton

This article is a contribution to the Topical Collection *Biodiversity in Abyssal Polymetallic Nodule Areas*

✉ Katja Uhlenkott
katja.uhlenkott@senckenberg.de

¹ German Centre for Marine Biodiversity Research (DZMB), Senckenberg Am Meer, Wilhelmshaven, Germany

² Marine Biodiversity Research, Institute for Biology and Environmental Sciences, Carl Von Ossietzky University, Oldenburg, Germany

³ National Oceanography Centre, Southampton, UK

⁴ Federal Institute for Geosciences and Natural Resources (BGR), Hannover, Germany

and Barry 2010) and, to a lesser extent, abyssal plains (e.g. Durden et al. 2015; Kaiser et al. 2017; Simon-Lledó et al. 2020). In the CCZ, habitat heterogeneity arises at different scales (e.g. Simon-Lledó et al. 2020). Regionally, water depth increases continuously from ca. 4000 m in the east to more than 5000 m in the west (GEBCO 2014), generally covarying with a respectively decreasing flux of particulate organic carbon (POC) from the sea surface (Lutz et al. 2007). Additionally, carbon supply exhibits a latitudinal gradient towards the more productive equatorial waters south of the CCZ. In addition to the average gradients in depth and POC-flux, bathymetric features such as seamounts and abyssal hills (Wedding et al. 2013; Uhlenkott et al. 2022), but also smaller depressions and elevations (Simon-Lledó et al. 2019b), contribute to increase habitat heterogeneity at more local scales.

This study focusses on the megafaunal assemblages on bathymetric elevations, including both the foothills of two seamounts and three abyssal hills. Following the definition by Yesson (2011), seamounts are defined as elevations of more than 1000 m compared to the surrounding abyssal plain in this study, abyssal hills are smaller elevations of only several hundreds of meters. In the CCZ, seamounts and the smaller abyssal hills have been described to harbour different megafaunal assemblages compared to the adjacent abyssal plains (Simon-Lledó et al. 2019b, 2020; Cuvelier et al. 2020). A similar pattern was also observed in Atlantic abyssal plains, in association with enhanced biomass at abyssal hills in comparison to the abyssal plain (Durden et al. 2015). On large seamounts, the most obvious shifts in faunal composition are commonly observed with variation in water depth, usually in response to changes in factors such as temperature, oxygen and food availability (Clark et al. 2010). Another factor, that has been described to influence food availability at seamounts (Rogers 2018) as well as abyssal hills (Morris et al. 2016) is the influence of these bathymetric elevations on the benthic current regime, which can locally lead to the trapping of food particles.

Another feature adding to habitat heterogeneity is the availability of hard substratum in the deep sea, which has been widely linked to increased habitat complexity on seamounts (McClain 2007; Clark et al. 2010; Rogers 2018) and more recently also in bathyal and abyssal areas (Riehl et al. 2020). Here, hard substratum can enhance diversity (Meyer et al. 2016) or induce substantial changes in benthic abundance and composition (Simon-Lledó et al. 2019b). In the CCZ, seamounts as well as abyssal hills of volcanic origin can harbour sites with basaltic rock outcrops covered with iron-manganese crusts (Kuhn et al. 2020). However, seamounts and abyssal hills are not to be considered as one continuous habitat, but consist of a mixture of rocky patches and soft-sedimented areas (e.g. Clark et al. 2010; Durden et al. 2015; Rogers 2018). Abyssal hills in the CCZ can also harbour high abundances of polymetallic nodules (e.g. Simon-Lledó et al. 2020), metallic conglomerates lying on the sediment surface

that are composed of many valuable metals such as copper, nickel, manganese and cobalt (Kuhn et al. 2017; Hein et al. 2020). Polymetallic nodules, especially in the abyssal plains of the CCZ, are thus of great economic interest, triggering exploration and investigation by multiple governmental and scientific agencies as well as private companies (Jones et al. 2017, 2021). However, nodules are also an essential source of hard substratum for many abyssal taxa in the CCZ (e.g. Amon et al. 2016; Vanreusel et al. 2016; Simon-Lledó et al. 2019b). As such, the availability of nodules and the presence of bathymetric elevations are thought to be key factors enhancing habitat heterogeneity and creating important ecological variations across space in the abyssal CCZ (Simon-Lledó et al. 2020).

Hard substratum is of special importance for sessile taxa that use the hard substratum as anchoring ground (e.g. Kersten et al. 2019) and as a platform to place their food-capturing structures in higher, accelerated boundary flows (Mullineaux 1989). The most abundant sessile megafaunal taxa of the CCZ typically include the coral taxa Alcyonacea and Actinaria, along with Porifera and Bryozoa, all showing different degrees of association with nodules (Amon et al. 2016; Vanreusel et al. 2016; Simon-Lledó et al. 2020). Additionally, certain life traits of mobile taxa can also require the presence of hard substratum. Incirrate octopods, for example, place their eggs on the stalks of dead sponges attached to polymetallic nodules (Purser et al. 2016). This high dependence on hard substratum has been flagged as a strong constrain for ecosystem recovery after mining disturbance (Simon-Lledó et al. 2019a), mostly owing to the lack of recolonization by sessile taxa in areas where nodules are removed (Jones et al. 2017).

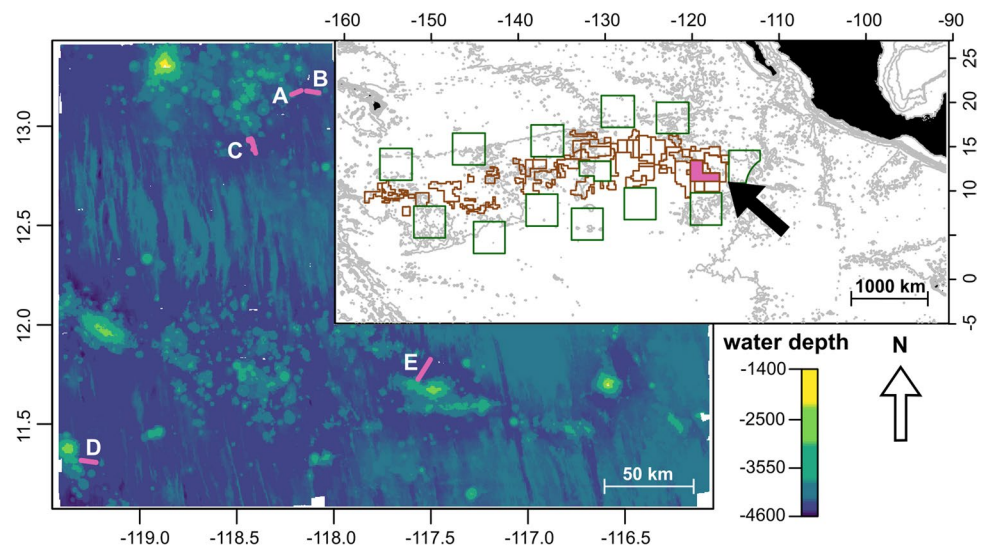
In this study, we have analysed photographic transects with megafauna at five different bathymetric elevations in the eastern CCZ, including three abyssal hills and two lower flanks of larger seamounts. In the context of habitat heterogeneity, we focused on:

- the spatial distribution of the habitats identifiable on images, i.e. the occurrence of rock, nodules and sediment;
- differences in megafaunal density and diversity between the habitats, and
- the identification of megafauna morphotypes mainly occurring in only one of the observed habitats.

Material and Methods

Five photographic transects were obtained within the eastern BGR (Federal Institute for Geosciences and Mineral Resources, Germany) (German) exploration contract area in the CCZ, all starting at a bathymetric elevation (seamount flank or abyssal hill) and moving downslope towards the abyssal plain (Fig. 1). They were obtained during three cruises on the research vessel SONNE in 2010 (SO-205),

Fig. 1 Bathymetric map of the eastern BGR contract area for the exploration of polymetallic nodules; magenta lines refer to the different towed camera transects conducted in the area (data: BGR) (left); and an overview map of the north-eastern Pacific between Hawaii and Mexico with the study area coloured in magenta and indicated by the arrow; brown lines indicate contractor areas for the exploration of polymetallic nodules, green lines areas of particular environmental interest (APEIs) (data: GEBCO 2014; International Seabed Authority 2020, 2021) (right)



2015 (SO-240) and 2018 (SO-261) (Table 1). The most southern transect (D) was obtained in 2010 with the Ocean Floor Observation System (OFOS) of the research vessel SONNE; during subsequent cruises the towed video-sledge STROMER of the BGR was used instead. In 2015, three transects (A, B & C) were obtained ~220 km north of transect D (Fig. 1). The fifth transect (E), obtained in 2018, was taken ~210 km north-eastwards of transect D (Fig. 1).

All images collected were scaled (i.e. seabed area calculated based on laser points distance) and georeferenced in accordance with towed-camera navigation data (Rühlemann and shipboard scientific party, 2010, 2019; Kuhn and shipboard scientific party 2015). One of two overlapping images was removed according to positioning and calculated area to avoid overlap and the subsequent risk of counting animals twice. To standardise animal detection only images covering <math>< 7 \text{ m}^2</math> (i.e. collected when the device was 2–4.5 m above the seabed) were used in the analysis, leading to a total number of 5304 images. Images were annotated using the BIIGLE annotation system (Langenkämper et al. 2017) as set up on the server of the Senckenberg Nature Research Society

(SGN) in accordance with an abyssal-Pacific standardised taxa catalogue compiled from previous image-based studies conducted in the region (see e.g., Simon-Lledó et al. 2019b, 2019c, 2019d) and existing literature (e.g. Amon et al. 2017; Molodtsova and Opresko 2017; Kersken et al. 2019). The taxonomic nomenclature of the morphotypes presented here follows Horton et al. (2021). Furthermore, images were classified into four different habitats in accordance with the seabed composition observed, i.e. rocky outcrops (abbreviated as “rock”), sediment covered with few nodules usually larger than 4 cm (abbreviated as “large nodules”), sediment covered with many nodules usually smaller than 4 cm (abbreviated as “small nodules”) and sediment areas free of nodules (abbreviated as “no nodules”) (Fig. 2). As nodules may partly be covered by sediment, nodule habitats were estimated from the image composition (Fig. 2). Only images assignable to one single habitat were used in habitat-based assessments, further reducing the dataset to 5016 images.

To investigate the spatial distribution of habitats, a dataset was compiled summarising images along the five transects into 20 m^2 subsamples. For each of these 20 m^2 subsamples, the predominant habitat was determined as the

Table 1 Meta-data of the photographic transects analysed for megafauna in this study. Both gears, the Ocean Floor Observation System (OFOS) and the STROMER (STR), are towed camera platforms

| Name (transect) | cruise | gear | year | length | number of images | seabed area | water depth | altitude difference | Water depth of nearest summit |
|-----------------|--------|------|------|---------|------------------|---------------------|-------------------|---------------------|-------------------------------|
| A (013_STR) | SO-240 | STR | 2015 | 6.5 km | 713 | 1.574 m^2 | 3.822 m – 4.364 m | 542 m | 3.738 m |
| B (028_STR) | SO-240 | STR | 2015 | 7.1 km | 1301 | 2.666 m^2 | 4.060 m – 4.320 m | 260 m | 4.048 m |
| C (041_STR) | SO-240 | STR | 2015 | 8.4 km | 394 | 755 m^2 | 3.897 m – 4.343 m | 446 m | 3.896 m |
| D (04_OFOS) | SO-205 | OFOS | 2010 | 13.2 km | 522 | 1.593 m^2 | 4.358 m – 4.423 m | 65 m | 3.513 m |
| E (168_STR) | SO-261 | STR | 2018 | 15.6 km | 2374 | 11.320 m^2 | 3.962 m – 4.377 m | 415 m | 3.431 m |

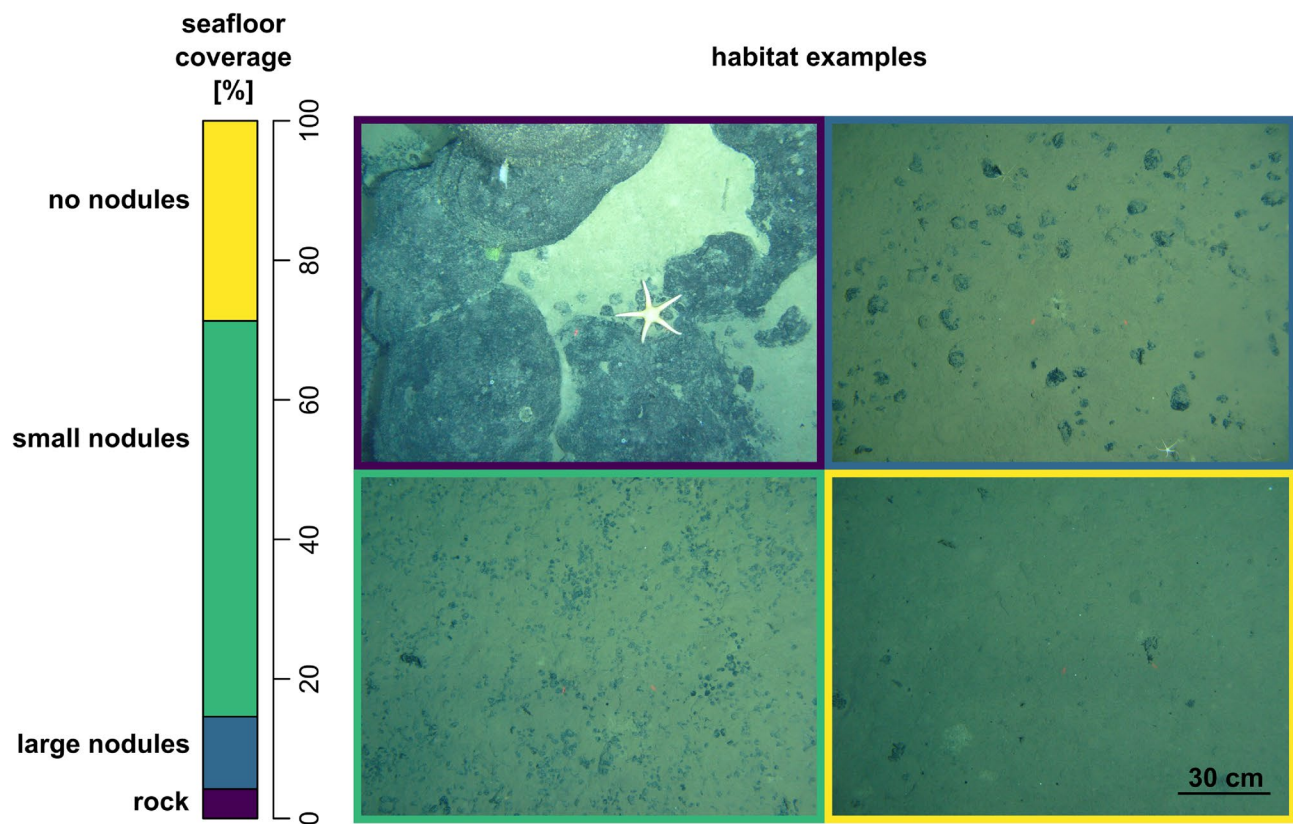


Fig. 2 Seafloor coverage of the four habitats occurring within the dataset and photographic examples of the four habitats defined as rock outcrop (top left), large polymetallic nodules (top right), small polymetallic nodules (bottom left) and sediment devoid of nodules (bottom right)

habitat proportionally covering the largest area of the 20 m² subsamples. Using this dataset of 20 m² subsamples, the random forest algorithm (Breiman 2001) as implemented in the R-package *randomForest* (Liaw and Wiener 2002) was applied to model and spatially predict the habitats using classification. Predictor data consisted of water depth and the seafloor backscatter value obtained using vessel-mounted swath echosounder systems, with a resolution of 121 m (Wiedicke-Hombach and shipboard scientific party 2009). The backscatter value provides information on the presence or absence of hard rock, the presence or absence

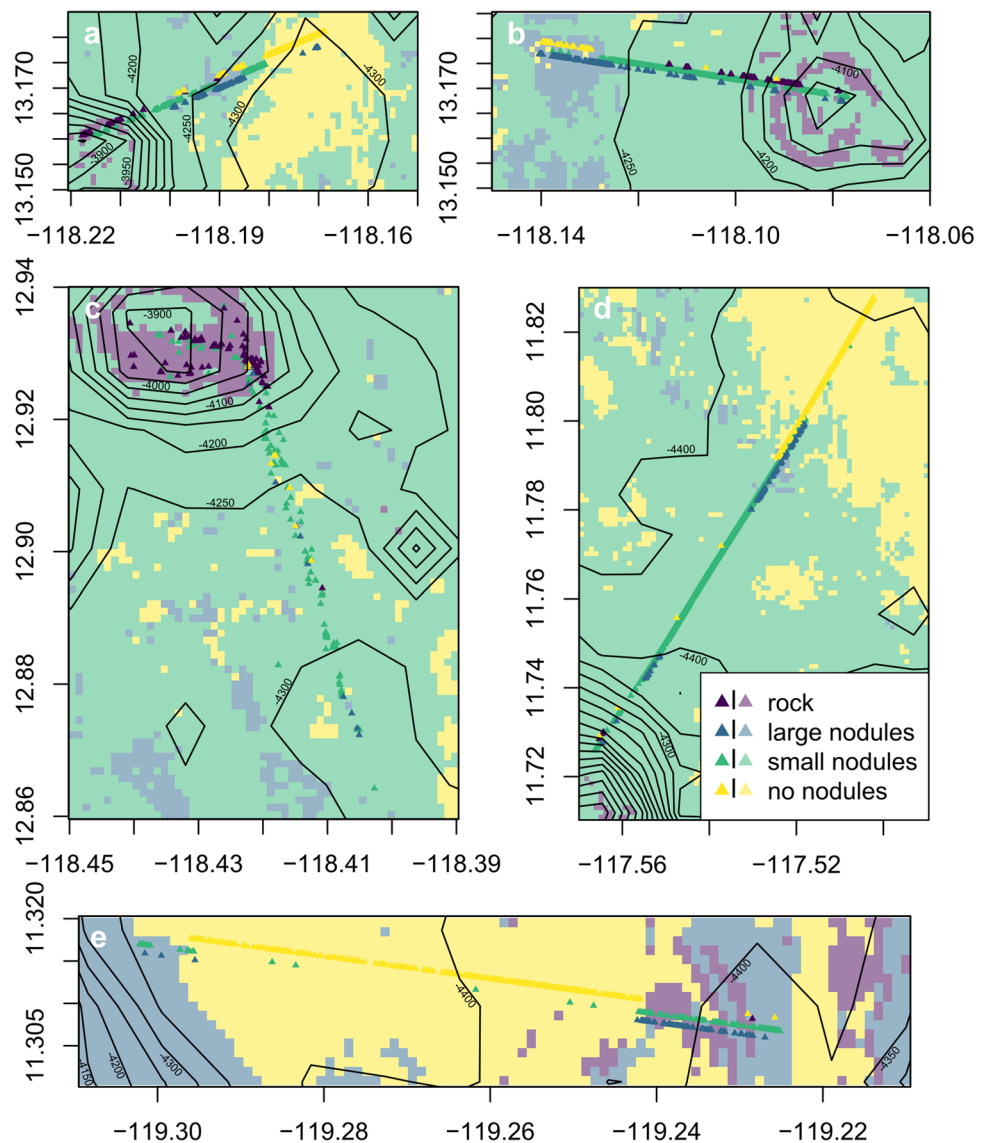
of nodules on sediment-covered abyssal plains as well as the dominating nodule size class in nodule fields (e.g. Kuhn et al. 2020). Based on water depth, the R-package *raster* (Hijmans 2020) was used to compute bathymetric characteristics (Table 2), which were also used as predictors.

Biodiversity and density of the megafauna in the different habitats were not investigated based on the 20 m² subsamples, but were compared based on 50 bootstrap samples of 100 individuals and 100 m² of seafloor coverage, respectively. Apart from morphotype density and morphotype richness, the biodiversity indices Simpson's Diversity Index (D)

Table 2 Bathymetric characteristics computed from water depth and used as predictor variables in the random forest models

| bathymetric characteristic | R-function | description |
|--|------------------|--|
| slope | <i>terrain()</i> | |
| northness | <i>terrain()</i> | aspect towards north |
| eastness | <i>terrain()</i> | aspect towards east |
| flow direction | <i>terrain()</i> | indication of deeper cells |
| bathymetric position index (0.3 km/1.5 km/5 km) | <i>focal()</i> | position (higher or deeper) in comparison to the mean depth of the surrounding area |
| terrain ruggedness index | <i>terrain()</i> | mean of difference of the position (higher or deeper) in comparison to surrounding cells |
| roughness | <i>terrain()</i> | difference of maximum and minimum in the surrounding of the position |

Fig. 3 Distribution of the different habitats predicted with random forest classification in the surroundings of **a** transect A; **b** transect B; **c** transect C; **d** transect E; **e** transect D; based on subsamples with an area of 20 m². Colours of the prediction maps as well as of the observational point data refer to the four different habitats with higher transparency in the predicted maps; the black lines represent depth isolines with an altitude difference of 50 m between lines



(Simpson 1949), Shannon's Diversity Index (H') (Shannon 1948) and Pielou's Evenness (J) (Pielou 1966) were applied. Morphotype distribution between habitats was compared using an UpSet plot (Gehlenborg 2019) based on the original dataset of 5016 images. Using the same dataset, the multinomial species classification method (CLAM) was used to identify potential specialists within the different habitats (Chazdon et al. 2011) by comparing observations from each habitat to the remaining dataset using the default settings of the function *clamtest*. If 2/3 or more of all occurrences of a morphotype are observed in one habitat, the morphotype is regarded as a predominantly present specialist. If the opposite is being observed, the morphotype is regarded as predominantly absent in this habitat. All of these computations were conducted in the statistical environment of R (R Core Team 2019) using the R-packages *vegan* (Oksanen et al. 2019) and *UpSetR* (Gehlenborg 2019).

Furthermore, the R-packages *reshape2* (Wickham 2007), *rangeBuilder* (Rabosky et al. 2016) and *viridisLite* (Garnier 2018) were used for data preparation and presentation.

Results

Distribution of habitats

The study area was divided into four different habitats, mainly being defined by the available hard substratum (Fig. 2). The most commonly observed habitat forming 56.7% of the study area comprises areas covered with small polymetallic nodules (predominantly < 4 cm diameter), which show a patchy distribution on top of the sediment (Fig. 2). Nodule-free sediment areas are the second-most abundant habitat, covering 28.7% of the study area (Fig. 2).

Table 3 Mean and standard deviation of morphotype richness, Shannon's diversity (H'), Simpson's diversity (D) and Pielou's Evenness (J) as well as megafauna density per m^2 computed from 50 bootstrapsamples for each habitat, either per 100 individuals or per 100 m^2 coverage of the seafloor

| habitat | rock | | large nodules | | small nodules | | no nodules | | all | |
|---------------|-------------|-------------|---------------|-------------|---------------|-------------|-------------|-------------|-------------|-------------|
| bootstrapping | 100 ind | 100 m^2 | 100 ind | 100 m^2 | 100 ind | 100 m^2 | 100 ind | 100 m^2 | 100 ind | 100 m^2 |
| richness | 29.1 ± 3.9 | 34.6 ± 4.4 | 32.2 ± 3.3 | 16.9 ± 3.22 | 34.2 ± 3.8 | 17.5 ± 3.6 | 29.0 ± 3.0 | 8.2 ± 2.0 | 36.0 ± 3.7 | 18.4 ± 3.6 |
| H' | 2.45 ± 0.22 | 2.53 ± 0.19 | 2.71 ± 0.15 | 2.37 ± 0.22 | 2.87 ± 0.19 | 2.46 ± 0.26 | 2.56 ± 0.17 | 1.84 ± 0.26 | 3.03 ± 0.16 | 2.59 ± 0.25 |
| D | 0.84 ± 0.04 | 0.84 ± 0.03 | 0.88 ± 0.02 | 0.86 ± 0.04 | 0.89 ± 0.03 | 0.86 ± 0.05 | 0.85 ± 0.03 | 0.79 ± 0.06 | 0.91 ± 0.02 | 0.89 ± 0.04 |
| J | 0.73 ± 0.04 | 0.71 ± 0.04 | 0.78 ± 0.03 | 0.85 ± 0.04 | 0.81 ± 0.04 | 0.86 ± 0.05 | 0.76 ± 0.04 | 0.88 ± 0.06 | 0.85 ± 0.03 | 0.89 ± 0.04 |
| density | 1.40 ± 0.24 | 1.39 ± 0.20 | 0.42 ± 0.05 | 0.39 ± 0.09 | 0.34 ± 0.05 | 0.34 ± 0.07 | 0.15 ± 0.02 | 0.15 ± 0.04 | 0.34 ± 0.05 | 0.34 ± 0.07 |

Large polymetallic nodules (predominantly > 4 cm diameter) characterise 10.4% of the area investigated in this study (Fig. 2). Compared to small nodules, the large nodules have a less patchy appearance and show a generally lower coverage of the sediment surface (Fig. 2). Finally, rock outcrop presents the smallest proportion of the dataset (4.2%), being mainly characterised by pillow lava covered with iron-manganese crusts and interlaced with sediment patches (Fig. 2).

Spatially, rock outcrop was most commonly observed at the highest elevations (most shallow water depths) of each of the transects A, B and C (Fig. 3a, b and c) and is, hence, also mainly predicted by random forest for the summits of those elevations (Fig. 3). The only exception is transect D, for which rock outcrop is also predicted to occur at a slight elevation within the abyssal plain (Fig. 3e). Transect D is also the only transect for which no coverage with small nodules is predicted in the surroundings of the elevation, although the observations suggest a mixture of small and large nodules in the area (Fig. 3e). In all other transects, the summits are predicted to be surrounded by areas covered with small nodules, which is predicted to be the prevalent habitat (Fig. 3a-d). Nodule-free sites occur at a distance of several kilometres from the summits in all transects except for transect C (Fig. 3c). This is also reflected in the spatial predictions except for transect B, where the nodule-free area is masked by the occurrence of large nodules (Fig. 3b).

Density and diversity of megafauna

Across the whole dataset, the average density of megafauna amounts to 0.34 ± 0.07 individuals per m^2 , independent of whether the density is computed from datasets of 100 individuals or per 100 m^2 of seafloor (Table 3). Comparing the different habitats, megafauna density is lowest in nodule-free areas (0.15 ± 0.04 individuals per m^2) and highest in areas covered with rock outcrop ($1.39\text{--}1.40 \pm 0.24$ individuals per m^2) (Table 3). In areas covered with nodules, average density is close to the overall density in areas with small nodules (0.34 ± 0.07 individuals per m^2), whereas it is slightly higher in areas with large nodules ($0.39\text{--}0.42 \pm 0.09$ individuals per m^2) (Table 3).

Computed richness and diversity vary if computations are based on spatial subsets or on fixed numbers of individuals (Table 3). Especially richness and Shannon's diversity (H') are highest in rock-covered areas compared to nodule-covered sites or nodule-free areas, when computations are based on subsets of 100 m^2 (Table 3). However, when based on subsets of 100 individuals, richness is highest in areas covered with small nodules, followed by large nodules (Table 3). In nodule-free and rock-covered areas, richness is comparably low, and diversity is even lowest in rock-covered areas (Table 3).

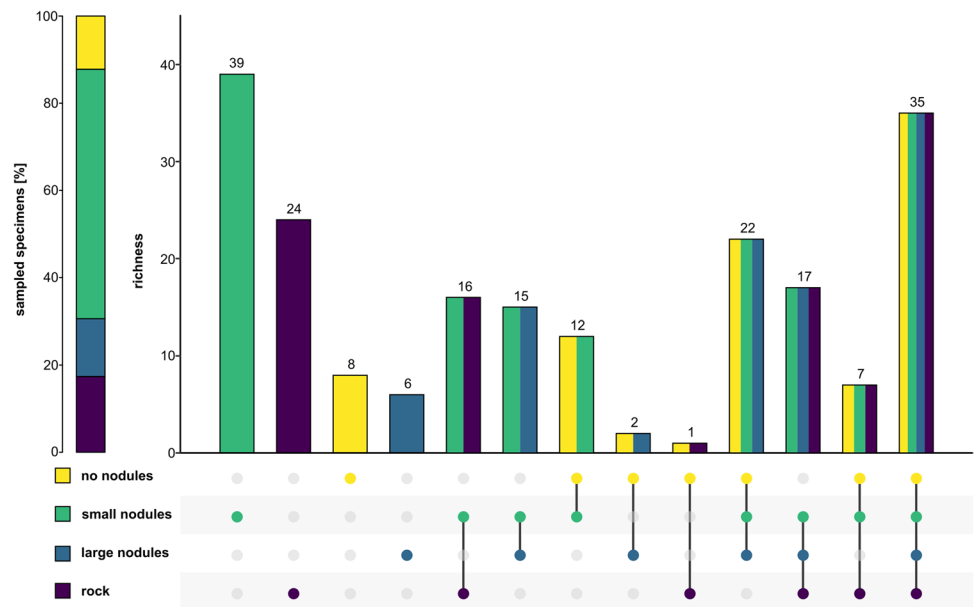
Simpson's diversity (D) and Pielou's evenness appear to be less influenced by megafauna density, although Simpson's diversity is still low in nodule-free sites (Table 3). Evenness, however, is especially low in rock areas, which is even more pronounced if the computations are based on a spatially defined area (Table 3). The values for richness, diversity and evenness are highest when regarding the whole dataset as a community (i.e. as one meta-habitat) (Table 3), thereby implying distinct faunal assemblages within the different habitats.

Investigating the habitats, the highest number of morphotypes exclusively observed in one habitat amounts to 39 morphotypes (19.9%) in the areas covered with small nodules (Fig. 4). However, the highest numbers of specimens were also obtained from this area (57.2%), whereas the areas covered with rock outcrops only formed 17.4% of all specimens, but 12.2% of all morphotypes (24) were found exclusively in this habitat (Fig. 4). The area devoid of nodules only comprises 8 exclusive morphotypes and also contains the lowest number of specimens (12.2%) (Fig. 4). Still, the highest number of morphotypes occurs when considering multiple habitats, and most of the observed morphotypes tend to occur in areas covered with small nodules, which also comprises the largest part of the dataset (Fig. 4).

Specialist and generalist morphotypes

Using the multinomial species classification method (CLAM) to further investigate morphotypes that are significantly more often observed within one of the habitats, the

Fig. 4 Bar plot representing the amount of specimens (in %) analysed in each of the four habitat types (left), and UpSet diagram showing the number of shared and unique morphotypes between/within the four habitats (right). Number of morphotypes = 196



majority of all morphotypes (77–89%) is regarded as being too rare to be defined as a generalist or specialist (Table 4). The largest amount of potential generalist morphotypes are obtained when the dataset is divided into small nodule areas versus other habitats (Table 4). However, this might be linked to the large amount of data associated with this habitat, enabling a more balanced analysis. Still, four morphotypes per habitat are suggested to be potential specialists, except for in the large nodule areas (Table 4). In this habitat, no specialists are suggested (Table 4).

Three morphotypes were recognised as generalists in all four habitats, all of these being most abundant in areas covered with small nodules, thus mirroring the abundance of habitats across the dataset (Table 5). Two of these morphotypes are sessile, the alcyonacean soft corals *Callozostrom bayeri* Cairns, 2016 sp. inc. (ALC_009; Fig. 5a) and Primnoidae gen. indet. (ALC_038; Fig. 5b), whereas Ophiuroidea order indet. mtp-OPH_022 is a mobile taxon.

The most abundant specialist morphotypes were the echinoderm morphotypes *Hymenaster* Wyville Thompson, 1873 sp. indet. mtp-AST_017 (Fig. 6a) and Ophiopyrgidae gen.

indet. (OPH_003; Fig. 6b) occurring at sites characterised by the presence of rock outcrops (Table 5). The two other sessile morphotypes associated with rock outcrops, the bryozoan Cyclostomatida fam. indet. (BRY_007; Fig. 6c) and the cup coral Deltocyathidae gen. indet. (SCL_002; Fig. 6d) occurred in lower numbers and were regarded as too rare by CLAM when investigating the other habitats (Table 5).

The most abundant morphotypes assigned as specialists to areas covered with small nodules were characterised as generalists in other areas. The bryozoan *Columnella* Levinsen, 1909 sp. indet. (BRY_003; Fig. 6e) is regarded as a generalist morphotype in areas with rock outcrop and large nodules, whereas the echinoid *Plesiodiadema globulosum* ((A. Agassiz, 1898) sp. inc. (URC_003; Fig. 6h) is assigned as a generalist in areas without nodule coverage as well as in areas with large nodules (Table 5). However, the number of specimens in the small nodule areas is much higher than the occurrences in all other areas. The holothurian *Synallactes* Ludwig, 1894 sp. indet. (HOL_104; Fig. 6g), on the other hand, was only found at small nodule sites, and the bryozoan Cyclostomatida fam. indet. (BRY_009; Fig. 6f) was seen

Table 4 Number and percentage of morphotypes that are recognised by the multinomial species classification method (CLAM) as being generalists, predominantly present specialists, predominantly absent specialists or rare in each of the four habitats

| habitat | rock | | large nodules | | small nodules | | no nodules | |
|----------------------|------|----|---------------|----|---------------|----|------------|----|
| | n | % | n | % | n | % | n | % |
| generalist | 17 | 8 | 20 | 10 | 39 | 19 | 12 | 6 |
| specialist (absent) | 7 | 3 | 2 | 1 | 5 | 3 | 6 | 3 |
| specialist (present) | 4 | 2 | 0 | 0 | 4 | 2 | 4 | 2 |
| too rare | 176 | 86 | 182 | 89 | 156 | 77 | 182 | 89 |

Table 5 Number of registered occurrences per habitat for the twelve morphotypes recognised by the multinominal species classification method (CLAM) as specialist morphotypes due to their predominance in one habitat, as well as generalists recognised in all habitats.

* recognised as present specialist in this habitat; () recognised as generalist in this habitat; recognised as rare in this habitat; n recognised as rare in this habitat

| morphotype | rock | large nodules | small nodules | no nodules | |
|--|------|---------------|---------------|------------|------------|
| <i>Hymenaster</i> sp. indet. mtp-AST_017 | 248* | 0 | 1 | 0 | specialist |
| Ophiopyrgidae gen. indet. mtp-OPH_003 | 261* | 0 | 3 | 0 | |
| Cyclostomatida fam. indet. mtp-BRY_007 | 16* | ± | ± | ∅ | |
| Deltocyathidae gen. indet. mtp-SCL_002 | 21* | ∅ | ∅ | ∅ | |
| <i>Columnella</i> sp. indet. mtp-BRY_003 | (7) | (12) | 111* | 1 | |
| Cyclostomatida fam. indet. mtp-BRY_009 | ∅ | ± | 36* | ± | |
| <i>Synallactes</i> sp. indet. mtp-HOL_104 | ∅ | ∅ | 18* | ∅ | |
| <i>Plesiadiadema globulosum</i> sp. inc. (URC_003) | 5 | (20) | 224* | (14) | |
| Hormathiidae gen. indet. mtp-ACT_022 | (3) | (7) | (24) | 36* | |
| Paxillosida fam. indet. mtp-AST_004 | 4 | (19) | 44 | 226* | |
| <i>Synallactes</i> sp. indet. mtp-HOL_007 | 0 | (3) | (18) | 26* | |
| Ophiuroidea order indet. mtp-OPH_015 | (2) | (4) | (17) | 30* | |
| <i>Callozostxon bayeri</i> sp. inc. (ALC_009) | 19 | 58 | 109 | 18 | generalist |
| Primnoidae gen. indet. mtp-ALC_038 | 45 | 21 | 129 | 17 | |
| Ophiuroidea order indet. mtp-OPH_022 | 5 | 17 | 48 | 6 | |

only three times outside of the small nodule areas (Table 5). Hence, these two morphotypes are regarded as too rare for assignment by CLAM in all areas except for the small nodule areas (Table 5).

Regarding the nodule-free sites, the asteroid Paxillosida fam. indet. (AST_004; Fig. 6j) is most clearly assigned to this area as a specialist, although it was classified as a generalist in areas with large nodules (Table 5). The holothurian *Synallactes* sp. indet. (HOL_007; Fig. 6k) does not occur at rocky sites but is regarded as a generalist at the nodule sites, despite the elevated occurrence in nodule-free sites (Table 5). The other two morphotypes, the anemone Hormathiidae gen. indet. (ACT_022; Fig. 6i) and the brittlestar Ophiuroidea order indet. (OPH_015; Fig. 6l), are only regarded as specialists in nodule-free sites; in all other habitats they are regarded as generalist morphotypes (Table 5).

Discussion

Influence of habitat heterogeneity on megafauna

Biodiversity is high in the abyss with regards to all size classes (Amon et al. 2016; Hauquier et al. 2019; Bonifácio et al. 2020; Uhlenkott et al. 2021; Washburn et al. 2021), possibly due to a much greater habitat heterogeneity than was previously thought (Durden et al. 2015; Riehl et al. 2020; Simon-Lledó et al. 2020). In the CCZ, heterogeneity can be observed on different levels including bathymetric features such as seamounts and abyssal hills, troughs and plains (Simon-Lledó et al. 2019b; Cuvelier et al. 2020), varying sedimentation rates (Volz et al. 2018) and varying size and abundance in polymetallic nodule coverage on the seafloor (Kuhn et al. 2020). In our study area in the

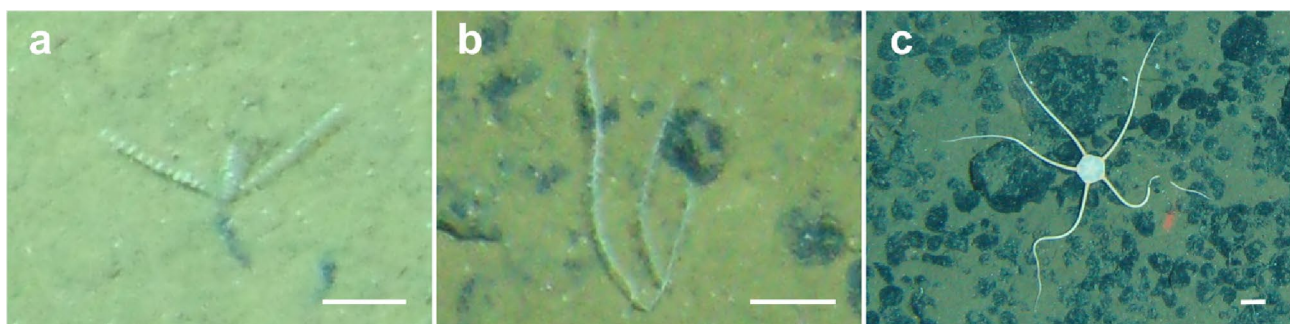


Fig. 5 Images of the morphotypes recognised as generalists by the multinominal species classification method (CLAM); **a** *Callozostxon bayeri* sp. inc. mtp-ALC_009; **b** Primnoidae fam. indet. mtp-ALC_038 and; **c** Ophiuroidea order indet. mtp-OPH_022; scale bars represent 2 cm

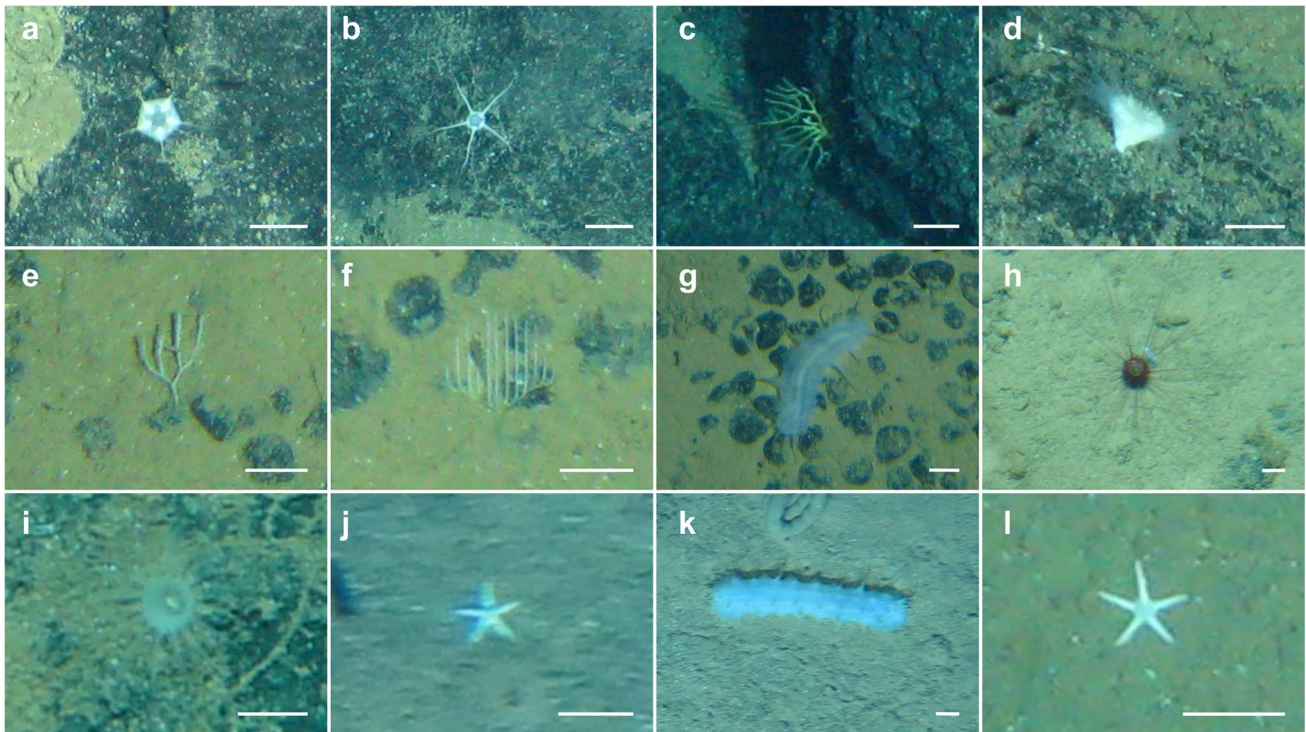


Fig. 6 Images of the morphotypes recognised as specialists by the multinomial species classification method (CLAM) for areas characterised by rock outcrop: **a** *Hymenaster* sp. indet. mtp-AST_017; **b** Ophiopyrgidae gen. indet. mtp-OPH_003; **c** Bryozoa class indet. mtp-BRY_007 and; **d** Deltocyathidae gen. indet. mtp-SCL_002; for areas with small nodules; **e** *Columnella* sp. indet. mtp-BRY_003;

f Bryozoa class indet. mtp-BRY_009; **g** *Synallactes* sp. indet. mtp-HOL_104 and **h** *Plesiadiadema globulosum* sp. inc. (URC_003), and for areas with no nodule coverage; **i** Hormathiidae gen. indet. mtp-ACT_022; **j** Paxillosida fam. indet. mtp-AST-004; **k** *Synallactes* sp. indet. mtp-HOL_007 and **l** Ophiuroidea order indet. mtp-OPH_015; scale bars represent 2 cm

eastern CCZ, the presence of a hard substratum on the seafloor appears to be in line with changes in megafauna and xenophyophore assemblages previously observed in abyssal-Pacific benthic communities (e.g. Gooday et al. 2017; Simon-Lledó et al. 2019c, 2020; Cuvelier et al. 2020).

In the part of the eastern CCZ studied here, areas with nodules on the seafloor sustained the highest benthic megafaunal diversity. From an ecological point of view, polymetallic nodules increase the seabed complexity in the abyssal plain, and thereby increase the number of available niches for the benthic community (Vanreusel et al. 2010). Although Vanreusel et al. (2010) refer to small-sized nematodes, the same reasoning may explain the higher biodiversity at sites with nodules compared to rock-covered and nodule-free areas. All three habitats contain patches of bare sediment, but only nodules and rock additionally provide hard substratum for megafauna. Comparing these substrates, the polymetallic nodules provide a much more complex surface structure than the relatively smooth pillow lavas, increasing the number of different niches and, hence, likely promoting a higher biodiversity.

Specimen-rarefied megafaunal assessments do not typically show variations in diversity across gradients of varying

nodule coverage of the seafloor, but rather changes in composition and faunal density (Simon-Lledó et al. 2019c, 2020). In our study, this pattern was also observed comparing areas with and without nodules, and might be related to higher food availability at nodule sites, as the greater roughness of the seafloor might act as a trap to accumulate particles. However, highest densities were found at sites with rock outcrops, combined with a decreased evenness compared to the other habitats. This can be explained by the dominance of large numbers of *Hymenaster* sp. indet. mtp-AST_017 and Ophiopyrgidae mtp-OPH_003, which our results suggest might be pillow-lava, rock-specific taxa.

Only a total of twelve specialist and three generalist morphotypes could be identified, as most morphotypes were too rare for an assignment given the characteristically low abundance of most benthic megafauna species in abyssal communities (e.g. Amon et al. 2016; Simon-Lledó et al. 2019b; Durden et al. 2021). While rare taxa can be essential for regional macroecology and beta diversity analysis (e.g. McGill et al. 2007), these are not expected to effectively contribute to the detection of habitat boundaries at local scales, unless of course they are not truly rare taxa (e.g. McClain 2021). Few observations of a certain morphotype may not

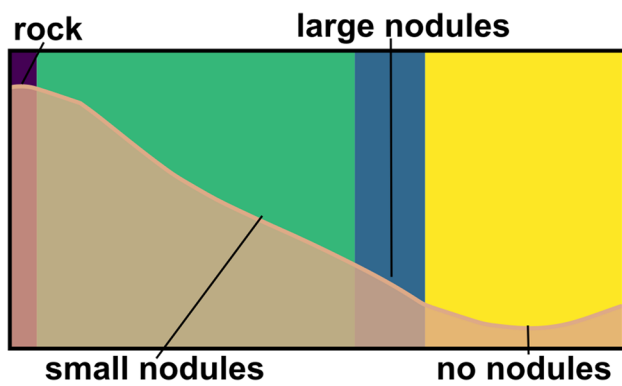


Fig. 7 Schematic representation of the habitat distribution at bathymetric elevations (seamounts and hills)

necessarily be regarded as real rarity, as they could well be an artefact of an insufficient sample size (Gotelli and Colwell 2001). It is likely, that we observed a similar pattern and that many morphotypes might indeed be generalists or specialists in our habitats.

In line with our results, most of the few studies that have so far compared megabenthic communities between seamounts or abyssal hills and adjacent abyssal plains (Durden et al. 2015, 2021; Simon-Lledó et al. 2019b; Cuvelier et al. 2020) have shown proportionally larger assemblage variations with increasing differences in depth. For instance, Cuvelier et al. (2020) showed that the density of *Callozostron bayeri*, a widely distributed soft coral in abyssal areas across the eastern CCZ (e.g. Amon et al. 2016; Simon-Lledó et al. 2019c, 2020), was up to 8 times higher on seamounts than in the adjacent nodule plains. In contrast, we have shown here that *Callozostron bayeri* sp. inc. (ALC_009) is one of the few generalist morphotypes and occurs most frequently in nodule areas, although it can also be observed at rock and nodule-free sites. The differences between the observations made by Cuvelier et al. (2020) and our results might be related to the larger depth gradient and the clearer distinction between seamount summit and seamount base in their study. The combined results from both studies show that local variations can be very important to contextualise regional patterns.

Spatial distribution of habitat heterogeneity

Although the elevations observed in this study vary distinctly in size and shape (Fig. 3), a similar pattern of habitat distribution can be observed at all sites (Fig. 7). Rock outcrop is mostly observed at the elevation summit, followed and interspersed by a terrain covered with small nodules. After a narrow band covered with large nodules, the elevation

is surrounded by an area devoid of nodules. For large seamounts, ring-like depressions at the base of the seamounts have been described, which are usually 100–200 m deeper than the surrounding abyssal plain and have been hypothesised to be the result of isostatic subsidence due to the continuous cooling and sinking of these seamounts (Kuhn et al. 2020). Due to the influences of seafloor elevations on currents and, hence, sedimentation processes (Mewes et al. 2014; Rogers 2018; Volz et al. 2018), sedimentation accumulation is thought to occur within these ring-like depressions. At smaller abyssal hills, where this phenomenon is not as pronounced, the base of the elevation might act as a sediment trap similar to the formation of a dune, preventing the formation of nodules, which can only form at sedimentation rates below 0.5 cm kyr^{-1} (Mewes et al. 2014).

The small layer of large nodules occurring at the rim of the nodule-free area and the occurrence of small nodules might be the result of a continuous increase in sedimentation from the top to the bottom of the elevation. In the study area, larger nodules, which are predominantly of diagenetic origin (i.e. obtain their minerals from porewater in the sediment), have been hypothesised to form at higher sedimentation rates compared to smaller nodules that are predominantly of hydrogenetic origin (i.e. obtain their minerals from bottom water) (Kuhn et al. 2020). The fact that the coverage with large nodules occurs in a relatively narrow transition zone could explain why no specialist morphotypes could be assigned to this habitat. Due to its occurrence between two other habitats (i.e. areas without nodule coverage and coverage with small nodules), this habitat might contain an intermediate megabenthic community, including common morphotypes from the areas covered with small nodules as well as from the nodule-free areas. Hence, a clear characterisation of specialists representative for this transitional habitat might be more difficult than comparing clearly separated habitats.

Additionally, this scheme might explain the difficulties arising from the prediction of habitats across transect D (Fig. 3e). This transect was obtained at the largest distance to the seamount summit and, hence, this is the only transect which had a relatively small difference in elevation from beginning to end ($< 100 \text{ m}$) and was sampled beyond the direct influence of the sinking seamount. Also, it might provide an explanation for the large differences in megafaunal communities commonly observed between the abyssal plain and bathymetric elevations (e.g. Durden et al. 2015; Cuvelier et al. 2020), although identical habitats do partly exist at both sites. For some species and morphotypes, the nodule-free sediment areas might decrease connectivity between nodule areas and, hence, lead to differences in the faunal composition of neighbouring nodule sites due to minor effects of islandness.

Conclusions

Increased habitat heterogeneity at the bathymetric elevations in the CCZ distinctly enhances megafaunal biodiversity. The highest biodiversity can be observed when regarding all habitats together (rock outcrops, areas with large nodules, areas with small nodules and areas without nodules) based on the same number of specimens or an area equal in size as if regarding a single habitat. Especially the inclusion of rock provides a habitat that is often overlooked in the CCZ, but that contains the most abundant and most clearly assigned specialist morphotypes observed during this study.

The distribution of habitats analysed by downslope photographic surveys in this study appears to be similar at different bathymetric elevations, although these include abyssal hills as well as the lower flanks of seamounts. At the summit, rock can be expected, followed by nodule-covered areas circumvented by nodule-free sediments. This structure might partly explain the large differences in megafaunal communities between bathymetric elevations and the abyssal plain observed in previous studies, even though very similar habitats occur in the plain and on selected parts of the elevations.

Acknowledgements We thank the captains and crew of the research vessel “Sonne” for their help and expertise during the scientific cruises “Mangan2010 (SO-205)”, “FLUM (SO-240)”, and “Mangan2018 (SO-262)”. We especially thank Marco Bruhn, Jutta Heitfeld, Franziska Iwan, Regina Posch, Tina Stein, Sven Hoffmann, Antje Fischer and Jennifer Stepler for their help annotating the deep-sea images. Additionally, we want to thank two anonymous reviewers for their valuable input.

Funding Open Access funding enabled and organized by Projekt DEAL. PMA and KU acknowledge funding by the German Federal Ministry of Education and Research (BMBF) as a contribution to the European JPI-Oceans projects “Ecological Aspects of Deep-Sea Mining” (grant number 03F0707E) and “Environmental Impacts and Risks of Deep-Sea Mining” (grant number 03F0812E). ESL received support from the NERC “Seabed Mining And Resilience To Experimental impact” (SMARTEx) project (Grant Reference NE/T003537/1).

Declarations

Conflict of Interest The authors declare that they have no conflict of interest.

Ethical approval No animal testing was performed during this study.

Sampling and field studies All necessary permits for sampling and observational field studies have been obtained by the authors from the competent authorities and are mentioned in the acknowledgements, if applicable. The study is compliant with CBD and Nagoya protocols.

Data availability The datasets analysed during the current study are available in the PANGAEA data publisher and information system, <https://doi.pangaea.de/10.1594/PANGAEA.946800>.

Author contributions KU, ESL and PMA conceived the ideas and designed the research. All authors collected the data. KU analysed the data. The first draft of the manuscript was written by KU and all

authors commented on previous versions of the manuscript. All authors read and approved the final manuscript.

Open Access This article is licensed under a Creative Commons Attribution 4.0 International License, which permits use, sharing, adaptation, distribution and reproduction in any medium or format, as long as you give appropriate credit to the original author(s) and the source, provide a link to the Creative Commons licence, and indicate if changes were made. The images or other third party material in this article are included in the article's Creative Commons licence, unless indicated otherwise in a credit line to the material. If material is not included in the article's Creative Commons licence and your intended use is not permitted by statutory regulation or exceeds the permitted use, you will need to obtain permission directly from the copyright holder. To view a copy of this licence, visit <http://creativecommons.org/licenses/by/4.0/>.

References

- Agassiz A (1898) Reports on the dredging operations off the west coast of Central America to the Galápagos, to the the west coast of México, and in the Gulf of California, in charge of Alexander Agassiz, carried on by the U.S. Fish Commission Steamer “Albatross”, during 1891, Lieut. Commander Z. L. Tanner, U.S.N., Commanding. XXIII. Preliminary report on the Echini. *Bull Mus comp Zol* 32:71–86
- Amon DJ, Ziegler AF, Dahlgren TG, Glover AG, Goineau A, Gooday AJ et al (2016) Insights into the abundance and diversity of abyssal megafauna in a polymetallic-nodule region in the eastern Clarion-Clipperton Zone. *Sci Rep* 6:30492. <https://doi.org/10.1038/srep30492>
- Amon DJ, Ziegler AF, Drazen JC, Grischenko AV, Leitner AB, Lindsay DJ, et al. (2017) Megafauna of the UKSRL exploration contract area and eastern Clarion-Clipperton Zone in the Pacific Ocean: Annelida, Arthropoda, Bryozoa, Chordata, Ctenophora, Mollusca. *Biodivers Data J*. 5, e14598. <https://doi.org/10.3897/BDJ.5.e14598>
- Bell JB, Alt CHS, Jones DOB (2016) Benthic megafauna on steep slopes at the Northern Mid-Atlantic Ridge. *Mar Ecol* 37:1290–1302. <https://doi.org/10.1111/maec.12319>
- Bonifácio P, MartínezArbizu P, Menot L (2020) Alpha and beta diversity patterns of polychaete assemblages across the nodule province of the eastern Clarion-Clipperton Fracture Zone (equatorial Pacific). *Biogeosciences* 17:865–886. <https://doi.org/10.5194/bg-17-865-2020>
- Breiman L (2001) Random forests. *Mach Learn* 45:5–32. <https://doi.org/10.1023/A:1010933404324>
- Cairns SD (2016) New abyssal Primnoidea (Anthozoa: Octocorallia) from the Clarion-Clipperton Fracture Zone, equatorial northeastern Pacific. *Mar Biodivers* 46(1):141–150. <https://doi.org/10.1007/s12526-015-0340-x>
- Chazdon RL, Chao A, Colwell RK, Lin S-Y, Norden N, Letcher SG et al (2011) A novel statistical method for classifying habitat generalists and specialists. *Ecology* 92:1332–1343. <https://doi.org/10.1890/10-1345.1>
- Clark MR, Rowden AA, Schlacher T, Williams A, Consalvey M, Stocks KI et al (2010) The Ecology of Seamounts: Structure, Function, and Human Impacts. *Annu Rev Mar Sci* 2:253–278. <https://doi.org/10.1146/annurev-marine-120308-081109>
- Cuvellier D, Ribeiro PA, Ramalho SP, Kersken D, MartínezArbizu P, Colaço A (2020) Are seamounts refuge areas for fauna from polymetallic nodule fields? *Biogeosciences* 17:2657–2680. <https://doi.org/10.5194/bg-17-2657-2020>
- Durden JM, Bett BJ, Huffard CL, Ruhl HA, Smith KL (2019) Abyssal deposit-feeding rates consistent with the metabolic theory of ecology. *Ecology* 100:e02564. <https://doi.org/10.1002/ecy.2564>

- Durden JM, Bett BJ, Jones DOB, Huvenne VAI, Ruhl HA (2015) Abyssal hills – hidden source of increased habitat heterogeneity, benthic megafaunal biomass and diversity in the deep sea. *Prog Oceanogr* 137:209–218. <https://doi.org/10.1016/j.pocean.2015.06.006>
- Durden JM, Putts M, Bingo S, Leitner AB, Drazen JC, Gooday AJ et al (2021) Megafaunal ecology of the western Clarion Clipperton Zone. *Front Mar Sci* 8:671062. <https://doi.org/10.3389/fmars.2021.671062>
- Garnier S (2018) viridisLite: Default color maps from “matplotlib” (version 0.3.0). Available at: <https://CRAN.R-project.org/package=viridisLite>.
- GEBCO (2014) The GEBCO_2014 Grid, version 20150318. Gen Bathymetr Chart Oceans. Available at: <http://www.gebco.net> [Accessed July 2, 2018]
- Gehlenborg N (2019) UpSetR: A more scalable alternative to Venn and Euler diagrams for visualizing intersecting sets (version 1.4.0). Available at: <https://CRAN.R-project.org/package=UpSetR>
- Gooday AJ, Holzmann M, Caille C, Goineau A, Kamenskaya O, Weber AA-T et al (2017) Giant protists (xenophyophores, Foraminifera) are exceptionally diverse in parts of the abyssal eastern Pacific licensed for polymetallic nodule exploration. *Biol Conserv* 207:106–116. <https://doi.org/10.1016/j.biocon.2017.01.006>
- Gotelli NJ, Colwell RK (2001) Quantifying biodiversity: procedures and pitfalls in the measurement and comparison of species richness. *Ecol Lett* 4:379–391. <https://doi.org/10.1046/j.1461-0248.2001.00230.x>
- Hauquier F, Macheriotou L, Bezerra TN, Egho G, MartínezArbizu P, Vanreusel A (2019) Distribution of free-living marine nematodes in the Clarion-Clipperton Zone: implications for future deep-sea mining scenarios. *Biogeosciences* 16:3475–3489. <https://doi.org/10.5194/bg-16-3475-2019>
- Hein JR, Koschinsky A, Kuhn T (2020) Deep-ocean polymetallic nodules as a resource for critical materials. *Nat Rev Earth Environ* 1:158–169. <https://doi.org/10.1038/s43017-020-0027-0>
- Hijmans RJ (2020) raster: Geographic data analysis and modeling (version 3.3-13). Available at: <https://CRAN.R-project.org/package=raster>
- Horton T, Marsh L, Bett BJ, Gates AR, Jones DOB, Benoist NMA et al (2021) Recommendations for the standardisation of open taxonomic nomenclature for image-based identifications. *Front Mar Sci* 8:620702. <https://doi.org/10.3389/fmars.2021.620702>
- International Seabed Authority (2020) Deep seabed mineral resources. <https://www.isa.org.jm/exploration-contracts/polymetallic-nodules>. Accessed 10 Mar 2020
- International Seabed Authority (2021) Decision of the Council of the International Seabed Authority relating to the review of the environmental management plan for the Clarion-Clipperton Zone. Kingston, Jamaica
- Jones DOB, Brewer ME (2012) Response of megabenthic assemblages to different scales of habitat heterogeneity on the Mauritanian slope. *Deep-Sea Res Pt I*. 67:98–110. <https://doi.org/10.1016/j.dsr.2012.05.006>
- Jones DOB, Kaiser S, Sweetman AK, Smith CR, Menot L, Vink A et al (2017) Biological responses to disturbance from simulated deep-sea polymetallic nodule mining. *PLOS ONE* 12:e0171750. <https://doi.org/10.1371/journal.pone.0171750>
- Jones DOB, Simon-Lledó E, Amon DJ, Bett BJ, Caille C, Clément L et al. (2021) Environment, ecology, and potential effectiveness of an area protected from deep-sea mining (Clarion Clipperton Zone, abyssal Pacific). *Prog Oceanogr* 197, 102653. <https://doi.org/10.1016/j.pocean.2021.102653>
- Kaiser S, Smith CR, MartínezArbizu P (2017) Editorial: Biodiversity of the Clarion Clipperton Fracture Zone. *Mar Biodivers* 47:259–264. <https://doi.org/10.1007/s12526-017-0733-0>
- Kersken D, Janussen D, MartínezArbizu P (2019) Deep-sea glass sponges (Hexactinellida) from polymetallic nodule fields in the Clarion-Clipperton Fracture Zone (CCFZ), northeastern Pacific: Part II—Hexasterophora. *Mar Biodivers* 49:947–987. <https://doi.org/10.1007/s12526-018-0880-y>
- Kuhn T, and shipboard scientific party (2015). SO240 FLUM: Low-temperature fluid circulation at seamounts and hydrothermal pits: heat flow regime, impact on biogeochemical processes, and its potential influence on the occurrence and composition of manganese nodules in the equatorial eastern Pacific. Hannover, Germany: Bundesanstalt für Geowissenschaften und Rohstoffe (BGR)
- Kuhn T, Uhlenkott K, Vink A, Rühlemann C, Martínez Arbizu P (2020) Manganese nodule fields from the Northeast Pacific as benthic habitats, in *Seafloor geomorphology as benthic habitat: GeoHab Atlas of seafloor geomorphic features and benthic habitats*, eds. P. T. Harris and E. Baker (Amsterdam, Netherlands: Elsevier), 933–947
- Kuhn T, Wegorzewski A, Rühlemann C, Vink A (2017) Composition, formation, and occurrence of polymetallic nodules, in *Deep-Sea Mining: Resource Potential, Technical and Environmental Considerations*, ed. R. Sharma (Cham, Switzerland: Springer International Publishing), 23–63. https://doi.org/10.1007/978-3-319-52557-0_2
- Langenkämper D, Zuerowietz M, Schoening T, Nattkemper TW (2017) BIIGLE 2.0 - Browsing and annotating large marine image collections. *Front Mar Sci* 4:83. <https://doi.org/10.3389/fmars.2017.00083>
- Levin LA, Sibuet M, Gooday AJ, Smith CR, Vanreusel A (2010) The roles of habitat heterogeneity in generating and maintaining biodiversity on continental margins: an introduction. *Mar Ecol* 31:1–5. <https://doi.org/10.1111/j.1439-0485.2009.00358.x>
- Levinsen GMR (1909) Morphological and systematic studies on the cheilostomatous Bryozoa. Nationale Forfatterers Forlag, Copenhagen, pp 1–431
- Liaw A, Wiener M (2002) Classification and regression by randomForest. *R News* 2:18–22
- Ludwig H (1894) The Holothurioidea. In: Reports on an exploration off the west coasts of Mexico, Central and South America, and off the Galapagos Islands, in charge of Alexander Agassiz, by the U. S. Fish Commission Steamer "Albatross," during 1891, Lieut. Commander Z. L. Tanner, U. S. N., commanding. XII. Memoirs of the Museum of Comparative Zoölogy at Harvard College. 17(3): 183
- Lutz MJ, Caldeira K, Dunbar RB, Behrenfeld MJ (2007) Seasonal rhythms of net primary production and particulate organic carbon flux to depth describe the efficiency of biological pump in the global ocean. *J Geophys Res Oceans* 112:C10011. <https://doi.org/10.1029/2006JC003706>
- MacArthur RH, MacArthur JW (1961) On bird species diversity. *Ecology* 42:594–598. <https://doi.org/10.2307/1932254>
- McClain CR (2007) Seamounts: identity crisis or split personality? *J Biogeogr* 34:2001–2008. <https://doi.org/10.1111/j.1365-2699.2007.01783.x>
- McClain CR (2021) The commonness of rarity in a deep-sea taxon. *Oikos* 130:863–878. <https://doi.org/10.1111/oik.07602>
- McClain CR, Barry JP (2010) Habitat heterogeneity, disturbance, and productivity work in concert to regulate biodiversity in deep submarine canyons. *Ecology* 91:964–976. <https://doi.org/10.1890/09-0087.1>
- McGill BJ, Etienne RS, Gray JS, Alonso D, Anderson MJ, Benecha HK et al (2007) Species abundance distributions: moving beyond single prediction theories to integration within an ecological framework. *Ecol Lett* 10:995–1015. <https://doi.org/10.1111/j.1461-0248.2007.01094.x>
- Mewes K, Mogollón JM, Picard A, Rühlemann C, Kuhn T, Nöthen K et al (2014) Impact of depositional and biogeochemical processes on small scale variations in nodule abundance in the Clarion-Clipperton Fracture Zone. *Deep-Sea Res Pt I* 91:125–141. <https://doi.org/10.1016/j.dsr.2014.06.001>

- Meyer KS, Young CM, Sweetman AK, Taylor J, Soltwedel T, Bergmann M (2016) Rocky islands in a sea of mud: biotic and abiotic factors structuring deep-sea dropstone communities. *Mar Ecol Prog Ser* 556:45–57. <https://doi.org/10.3354/meps11822>
- Molodtsova TN, Opresko DM (2017) Black corals (Anthozoa: Antipatharia) of the Clarion-Clipperton Fracture Zone. *Mar Biodivers* 47:349–365. <https://doi.org/10.1007/s12526-017-0659-6>
- Morris KJ, Bett BJ, Durden JM, Benoist NMA, Huvenne VAI, Jones DOB et al (2016) Landscape-scale spatial heterogeneity in phyto-detrital cover and megafauna biomass in the abyss links to modest topographic variation. *Sci Rep* 6:34080. <https://doi.org/10.1038/srep34080>
- Mullineaux LS (1989) Vertical distributions of the epifauna on manganese nodules: Implications for settlement and feeding. *Limnol Oceanogr* 34:1247–1262. <https://doi.org/10.4319/lo.1989.34.7.1247>
- Oksanen J, Blanchet FG, Friendly M, Kindt R, Legendre P, McGlinn D et al. (2019) *vegan: Community ecology package (version 2.5-6)*. Available at: <https://CRAN.R-project.org/package=vegan>
- Pielou EC (1966) The measurement of diversity in different types of biological collections. *J Theor Biol* 13:131–144. [https://doi.org/10.1016/0022-5193\(66\)90013-0](https://doi.org/10.1016/0022-5193(66)90013-0)
- Purser A, Marcon Y, Hoving H-JT, Vecchione M, Piatkowski U, Eason D et al (2016) Association of deep-sea incirrate octopods with manganese crusts and nodule fields in the Pacific Ocean. *Curr Biol* 26:R1268–R1269. <https://doi.org/10.1016/j.cub.2016.10.052>
- R Core Team (2019). R: A language and environment for statistical computing. Vienna, Austria: R Foundation for Statistical Computing (version 3.6.2). Available at: <https://www.R-project.org/>
- Rabosky ARD, Cox CL, Rabosky DL, Title PO, Holmes IA, Feldman A et al (2016) Coral snakes predict the evolution of mimicry across New World snakes. *Nat Commun* 7:1–9. <https://doi.org/10.1038/ncomms11484>
- Ramirez-Llodra E, Brandt A, Danovaro R, De Mol B, Escobar E, German CR et al (2010) Deep, diverse and definitely different: unique attributes of the world's largest ecosystem. *Biogeosciences* 7:2851–2899. <https://doi.org/10.5194/bg-7-2851-2010>
- Ramirez-Llodra E, Tyler PA, Baker MC, Bergstad OA, Clark MR, Escobar E et al (2011) Man and the last great wilderness: Human impact on the deep sea. *PLOS ONE* 6:e22588. <https://doi.org/10.1371/journal.pone.0022588>
- Rex MA, Etter RJ, Morris JS, Crouse J, McClain CR, Johnson NA et al (2006) Global bathymetric patterns of standing stock and body size in the deep-sea benthos. *Mar Ecol Prog Ser* 317:1–8. <https://doi.org/10.3354/meps317001>
- Riehl T, Wöfl A-C, Augustin N, Devey CW, Brandt A (2020) Discovery of widely available abyssal rock patches reveals overlooked habitat type and prompts rethinking deep-sea biodiversity. *Proc Natl Acad Sci* 117:15450–15459. <https://doi.org/10.1073/pnas.1920706117>
- Rogers AD (2018) Chapter Four - The Biology of Seamounts: 25 Years on, in *Advances in Marine Biology*, ed. C. Sheppard (Academic Press), 137–224 <https://doi.org/10.1016/bs.amb.2018.06.001>
- Rühlemann C, and shipboard scientific party (2010) SO205 MANGAN. Hannover, Germany: Bundesanstalt für Geowissenschaften und Rohstoffe (BGR)
- Rühlemann C, and shipboard scientific party (2019) MANGAN 2018. Hannover, Germany: Bundesanstalt für Geowissenschaften und Rohstoffe (BGR)
- Shannon CE (1948) A mathematical theory of communication. *Bell Syst Tech J* 27:379–423
- Simon-Lledó E, Bett BJ, Huvenne VAI, Köser K, Schoening T, Greinert J et al. (2019a) Biological effects 26 years after simulated deep-sea mining. *Sci Rep* 9:8040. <https://doi.org/10.1038/s41598-019-44492-w>
- Simon-Lledó E, Bett BJ, Huvenne VAI, Schoening T, Benoist NMA, Jeffreys RM et al (2019b) Megafaunal variation in the abyssal landscape of the Clarion Clipperton Zone. *Prog Oceanogr* 170:119–133. <https://doi.org/10.1016/j.pocean.2018.11.003>
- Simon-Lledó E, Bett BJ, Huvenne VAI, Schoening T, Benoist NMA, Jones DOB (2019c) Ecology of a polymetallic nodule occurrence gradient: Implications for deep-sea mining. *Limnol Oceanogr* 64:1883–1894. <https://doi.org/10.1002/lno.11157>
- Simon-Lledó E, Pomee C, Ahokava A, Drazen JC, Leitner AB, Flynn A et al (2020) Multi-scale variations in invertebrate and fish megafauna in the mid-eastern Clarion Clipperton Zone *Prog Oceanogr* 187:102405. <https://doi.org/10.1016/j.pocean.2020.102405>
- Simon-Lledó E, Thompson S, Yool A, Flynn A, Pomee C, Parianos J et al (2019d) Preliminary observations of the abyssal megafauna of Kiribati. *Front Mar Sci* 6:605. <https://doi.org/10.3389/fmars.2019.00605>
- Simpson EH (1949) Measurement of Diversity. *Nature* 163:688–688. <https://doi.org/10.1038/163688a0>
- Tews J, Brose U, Grimm V, Tielbörger K, Wichmann MC, Schwager M et al (2004) Animal species diversity driven by habitat heterogeneity/diversity: the importance of keystone structures. *J Biogeogr* 31:79–92. <https://doi.org/10.1046/j.0305-0270.2003.00994.x>
- Uhlenkott K, Simon-Lledó E, Vink A, MartínezArbizu P (2022) Investigating the benthic megafauna in the eastern Clarion Clipperton Fracture Zone (north-east Pacific) based on distribution models predicted with random forest. *Sci Rep* 12:8229. <https://doi.org/10.1038/s41598-022-12323-0>
- Uhlenkott K, Vink A, Kuhn T, Gillard B, MartínezArbizu P (2021) Meiofauna in a potential deep-sea mining area - Influence of temporal and spatial variability on small scale abundance models. *Diversity* 13:3. <https://doi.org/10.3390/d13010003>
- Vanreusel A, Fonseca G, Danovaro R, Silva MCD, Esteves AM, Ferrero T et al (2010) The contribution of deep-sea macrohabitat heterogeneity to global nematode diversity. *Mar Ecol* 31:6–20. <https://doi.org/10.1111/j.1439-0485.2009.00352.x>
- Vanreusel A, Hilario A, Ribeiro PA, Menot L, MartínezArbizu P (2016) Threatened by mining, polymetallic nodules are required to preserve abyssal epifauna. *Sci Rep* 6:26808. <https://doi.org/10.1038/srep26808>
- Volz JB, Mogollón JM, Geibert W, Arbizu PM, Koschinsky A, Kasten S (2018) Natural spatial variability of depositional conditions, biogeochemical processes and element fluxes in sediments of the eastern Clarion-Clipperton Zone, Pacific Ocean. *Deep-Sea Res Pt I* 140:159–172. <https://doi.org/10.1016/j.dsr.2018.08.006>
- Washburn TW, Menot L, Bonifácio P, Pape E, Błażewicz M, Bribiesca-Contreras G et al (2021) Patterns of macrofaunal biodiversity across the Clarion-Clipperton Zone: An area targeted for seabed mining. *Front Mar Sci* 8:626571. <https://doi.org/10.3389/fmars.2021.626571>
- Wedding LM, Friedlander AM, Kittinger JN, Watling L, Gaines SD, Bennett M et al (2013) From principles to practice: a spatial approach to systematic conservation planning in the deep sea. *Proc R Soc B Biol Sci* 280:20131684. <https://doi.org/10.1098/rspb.2013.1684>
- Wickham H (2007) Reshaping data with the reshape package. *J Stat Softw* 21:1–20. <https://doi.org/10.18637/jss.v021.i12>
- Wiedicke-Hombach M, and shipboard scientific party (2009) Campaign “MANGAN 2008” with R/V Kilo Moana. Hannover, Germany: Bundesanstalt für Geowissenschaften und Rohstoffe (BGR)
- Wyville Thompson C (1873) *The depths of the sea*. Macmillan, London, p 527
- Yesson C, Clark MR, Taylor ML, Rogers AD (2011) The global distribution of seamounts based on 30 arc seconds bathymetry data. *Deep-Sea Res Pt I* 58:442–453. <https://doi.org/10.1016/j.dsr.2011.02.004>